Biogeosciences Discuss., 11, 15019–15035, 2014
www.biogeosciences-discuss.net/11/15019/2014/
doi:10.5194/bgd-11-15019-2014

Biogeosciences Discussions
Open Access

Technical Note: Hyperspectral lidar time series of pine canopy physiological parameters

T. Hakala[1], O. Nevalainen[1], S. Kaasalainen[1], and R. Mäkipää[2]

[1]Finnish Geodetic Institute, Masala, Finland
[2]Finnish Forest Research Institute (METLA), Vantaa, Finland

Received: 9 June 2014 – Accepted: 25 September 2014 – Published: 23 October 2014

Correspondence to: T. Hakala (teemu.hakala@fgi.fi)

Published by Copernicus Publications on behalf of the European Geosciences Union.

Abstract

We present an empirical application of hyperspectral lidar for monitoring the seasonal and spatial changes in pine chlorophyll content and upscaling the accurate leaf-level chlorophyll measurements into branch and tree level. The results show the capability of the new instrument for monitoring the changes in the shape and physiology of tree canopy: the spectral indices retrieved from the hyperspectral point cloud agree with laboratory measurements of the chlorophyll content. The approach opens new prospects for replacing destructive and labor-intensive manual sampling with remote observations of tree physiology.

1 Introduction

The photosynthetic activity in tree canopy is an indicator of tree health. Vigorous trees with high foliar biomass and chlorophyll content have high carbon assimilation capacity. Stress in vegetation has been shown to induce changes in the photosynthetically-active pigments such as chlorophyll *a* and *b*. Therefore, the leaf chlorophyll content is an important indicator of the photosynthetic capacity as well as tree productivity and stress (Coops et al., 2003; Lausch et al., 2013).

The leaf properties and the distribution of chlorophyll and nutrients within a canopy vary as a function of time and space, and depending on the resource availability (Wang and Schjoerring, 2012; Peltoniemi et al., 2012). Seasonal changes in plant phenology and chlorophyll content are correlated to the CO_2 flux. For monitoring these seasonal variations, methods are needed for accurate and nondestructive chlorophyll estimation, both at the leaf and canopy level (e.g., Gond et al., 1999). Chlorophyll estimation with spectral remote-sensing has been implemented increasingly in a number of studies (e.g., Coops et al., 2003; Lausch et al., 2013), but improved resolution and more accurate 3-D position for the spectra are still being called for, to extend the accurate leaf-level measurement into canopy and stand level (cf. Gaulton et al., 2013). To

BGD
11, 15019–15035, 2014

investigate the spatial variation of the photosynthetic capacity and self-shading of photosynthetically active tissue, the canopy and branch structure must also be included in the measurement.

One way to provide simultaneous structural and spectral information is lidar combined with hyperspectral passive sensing (e.g., Thomas et al., 2006; Jones et al., 2010), but new applications using multi or hyperspectral laser scanning have increased quite recently. Hancock et al. (2012) demonstrated the potential of dual wavelength, large-footprint, spaceborne lidar to separate ground and canopy returns using the extra information contained in a spectral ratio to complement the canopy height from laser scanning. Three-dimensional (3-D) distributions of vegetation biochemical properties were measured with spectral indices developed for the Salford Advanced Laser Canopy Analyser (SALCA), which is also a dual-wavelength lidar (Gaulton et al., 2013). A similar approach was used in the Dual-Wavelength Echidna Lidar (DWEL) (Douglas et al., 2012). A multispectral canopy lidar has also been introduced for simultaneous retrieval of vegetation structure and spectral indices (Woodhouse et al., 2011). In this approach, a tunable laser operating at four wavelengths was used.

In this technical note, an application of the recently developed hyperspectral lidar instrument (Hakala et al., 2012) is presented for monitoring the seasonal and spatial changes in pine chlorophyll content. As a non-destructive method, the capability of the instrument to upscale the accurate leaf-level chlorophyll content measurements into branch and tree level has been investigated and validated with chemical analysis of chlorophyll content.

2 Materials and methods

Hyperspectral lidar (HSL) is a prototype laser scanning instrument (Hakala et al., 2012) utilizing a supercontinuum laser. White laser pulses are sent to a target and the reflected echoes are timed for distance. A spectrograph and an avalanche photodiode (APD) array connected to a high-speed digitizer are used to determine the

BGD
11, 15019–15035, 2014

spectrum of each returning echo by measuring the intensity of the echo at multiple wavelengths. Also the intensity of each transmitted laser pulse is measured and used to normalize the echo intensity. Current prototype configuration uses a 16 element APD array and an 8 channel digitizer, enabling us to measure at 8 different wavelength bands: 545, 641, 675, 711, 742, 778, 978, 1292 nm. A reference target with known reflectance (Spectralon) is measured from multiple distances and these data are used for calibrating the reflectance over the whole measurement range. The instrument and data processing presented in more detail in Hakala et al. (2012).

A Scots pine (*Pinus sylvestris* L.) was scanned five times during the 2013 growth season. The tree was approximately 13 years old, 5.5 m high and it was growing in a small forest stand near the institute building. The HSL was mounted on a portable cart, and the tree was scanned from two directions. The scans were co-registered using white spherical reference targets placed on fixed locations on the target area. The distance between the scanner and the tree was about 5 m. The tree was scanned with 0.1° horizontal and about 0.02° vertical resolution and the resulting point clouds contained 200 000–470 000 echoes from the tree. The beam diameter at the target was about 5 mm.

Needle samples were taken immediately after the scan for laboratory analysis. Six branches were selected and the samples were taken from these branches according to needle cohorts (current year needles, and 1, 2, and 3 years old needles). Analysis of the chlorophyll contents followed the protocol described in Wellburn (1994) for extraction with dimethyl-sulfoxide (DMSO). After extraction, the chlorophyll concentrations were determined from solvents spectrophotometrically using wave-lengths 480.0, 649.1 and 665.1 nm (resolution 0.1–0.5 nm).

Two of the six sampled branches were clearly identifiable from the HSL point cloud, having enough point density and long enough growth of the branch. Parts of the branches that carried previous year needles were selected for further analysis, since they had needles present during all measurements. The parts of the point cloud

BGD
11, 15019–15035, 2014

containing the selected branch parts were isolated in post processing. Three spectral indices were tested for determining chlorophyll content of the needles.

The modified chlorophyll absorption ratio index using reflectance at 705 and 750 nm (referred here as MCARI750) was first presented by Wu et al. (2008). Contrary to the original MCARI (Daughtry et al., 2000), MCARI750 uses reflectance at 705 and 750 nm, which have shown better sensitivity to high chlorophyll contents (Wu et al., 2008). MCARI has been designed to measure the depth of the maximum chlorophyll absorption at 670 nm relative to green reflectance peak at 550 nm and reflectance at 700 nm, at canopy scale (Daughtry et al., 2000).

$$\text{MCARI750} = \left[(R_{750} - R_{705}) - 0.2 \cdot (R_{750} - R_{550})\right] \cdot \left(R_{750}/R_{705}\right) \quad (1)$$

The modified simple ratio (MSR), developed by Chen (1996), strives to have low noise effect and good linearity to vegetation biophysical parameters. MSR has been used to estimate chlorophyll and Leaf Area Index (LAI) at canopy scale. Wu et al. (2008) also developed MSR using reflectance at 705 and 750 nm, referred here as MSR2.

$$\text{MSR2} = \frac{R_{750}/R_{705} - 1}{\sqrt{R_{750}/R_{705} + 1}} \quad (2)$$

The Simple Ratio (SR) indices directly compare the reflectance and absorbance peaks of chlorophyll pigments, which make them sensitive to changes in chlorophyll content (Wu et al., 2008). Variety of wavelength combinations are used with simple ratio indices, but the one selected for this study is SR6 (Zarco-Tejada et al., 2001). It has been used to estimate chlorophyll at leaf level.

$$\text{SR6} = \frac{R_{750}}{R_{710}} \quad (3)$$

Additionally, normalised difference vegetation index (NDVI) (Rouse et al., 1973) was used to separate needles from branches. NDVI is the most widely used vegetation

BGD
11, 15019–15035, 2014

index. It is based on the contrast between high absorption at red and high reflectance at near-infrared (NIR). NDVI has been developed for canopy scale and it has been used for both chlorophyll and LAI estimation.

$$\mathrm{NDVI} = \frac{R_{800} - R_{670}}{R_{800} + R_{670}} \quad (4)$$

As the channels of the prototype HSL are limited to eight separate spectral bands, these indices had to be used with the closest available spectral band.

3 Results

The overall shape of the tree and changes in shape from May to November can be observed in Fig. 1 where no spectral information is used. The changes in the shape and the spectra of tree parts are visible in the spectral point clouds. To demonstrate this, we plot the time series of the NDVI over the pine branch from 15 May to 6 November 2013 in Fig. 2. The outbreak and growth of new shoots (May–June 2013) can be observed, as well as the year 2 parts drying out (September–October 2013) and falling off (November 2013).

To validate the capability of the HSL to estimate the chlorophyll content using spectral indices, we compared the HSL data with laboratory analysis over the growing season. We present data for two branches, denoted M2 and M3, which were best visible in the HSL point clouds. The trends in the chlorophyll content and the indices MCARI750, MSR2, and SR6 from HSL data are well reproduced for the individual branches (Figs. 3–5). For all three indices, the sample branch M2_1 (year 1 part of M2) was best correlated with the laboratory measurements with R^2 0.8–0.9. The R^2 for MCARI750 and MSR2 for M3_1 was 0.7, whereas SR6 performed worse for M3_1 (R^2 0.5). When the data from M2_1 and M3_1 were combined for regression, MCARI750 and MSR2 correlated with the chlorophyll content measured in the laboratory, whereas there was distinct difference in SR6 value levels for M2_1 and M3_1 (Fig. 6). The results were

BGD
11, 15019–15035, 2014

worse for indices averaged over the entire tree point cloud (the right column in Figs. 3–5), compared with the average of all year 1 needles measured in the laboratory. This is very likely a result of the variation of the physiological conditions between the tree parts, which is more pronounced when the sampling has been carried out over the entire tree (i.e., the point cloud), rather than just a few needle samples (as in the laboratory experiment). All in all, the analysis of branch parts shows that the spatial distribution of the HSL spectral indices describes the chlorophyll content within the branch, although more measurements are needed to better validate the results.

In Figs. 3–5, branch M2 and M3 laboratory measurements consist of two separate needles only. More sampling should have been performed, however, the number of needles in each branch part is limited and the tree had to be sampled several times during the year (this emphasizes the need for non-destructive methods). The number of laser echoes from year 0 and 2 were highly varying; in the first lidar point clouds the year 0 growths were very small providing very few echoes, and the year 2 and older growths started dropping needles before September measurement thus reducing the number of echoes during autumn compared to spring. If the laboratory measurements of all needles would have been used, the weight of the year 0 and 2 laboratory measurements would have been higher compared to the lidar point cloud. Some lidar echoes still originate from the year 0 and 2 needles, reducing the overall correlation between laboratory and lidar data for the whole tree.

The change in the shape of the tree point cloud is visible in Fig. 1. The fact that tree shape can be retrieved from HSL point clouds has been shown before in numerous studies (see Kaasalainen et al., 2014 and references therein). We have also shown in our previous study that the tree shape and its changes can be quantified from laser scanner point clouds using quantitative tree structure modelling (Kaasalainen et al., 2014). As the scope of this note was to show the added value of spectral data in the chlorophyll distribution monitoring, the changes in tree shape will be an object of our future study.

BGD
11, 15019–15035, 2014

4 Conclusions

We have shown that the hyperspectral lidar provides an empirical approach for efficient mapping the spatial distributions of tree physiological parameters that are correlated to reflectance of the foliage (such as chlorophyll *a* and *b*). Because the measurement is non-destructive, it can be repeated for the same target to produce time series of important tree functions, such as moisture condition, photosynthetic capacity, or physiological status.

We demonstrated that the seasonal changes in the shape and physiology of tree parts are visible in 3-D; parameters affecting tree physiology can be quantified with spectral indices and linked to a specific location in the tree canopy using the HSL point cloud. We validated the method with reference measurements of chlorophyll *a* and *b* concentration in a laboratory. According to our results hyperspectral lidar can be used for the monitoring of the chlorophyll content, but similarly, the approach has potential in the monitoring of the water, carotenoid or lignin content, which all affect reflectance of the foliage (Austin and Ballare, 2010).

The tree was scanned from two directions only. Increasing the number of scans from different directions around the tree will improve the results by increasing the point coverage. This will require some instrument development to allow a more efficient field use. Increasing the point density is also an important object of instrument improvement. However, the prototype instrument was capable of showing the potential of 3-D spectral measurements.

Further work is needed to find the best spectral indices for different applications (e.g., monitoring the effects of drought or limited amount of light on the physiology of different tree parts), and then optimize the spectral channels to match with these indices. This will improve the precision of the results. Increasing the number of spectral channels would also improve the channel optimization and efficiency. Once the approach is well established and calibrated, it has potential for replacing a number of laborious and destructive manual experiments, and hence providing a new tool for remote

BGD
11, 15019–15035, 2014

observations of tree physiology. Although the first results show the potential of the approach, further studies on the laser interaction with the canopy are needed to establish the method physically.

Acknowledgements. This study was funded by the Academy of Finland research projects "New techniques in active remote sensing: hyperspectral laser in environmental change detection" and "Mobile hyperspectral laser remote sensing".

References

Austin, A. T. and Ballaré, C. S.: Dual role of lignin in plant litter decomposition in terrestrial ecosystems. P. Natl. Acad. Sci. USA, 107, 4618–4622, doi:10.1073/pnas.0909396107, 2010.

Chen, J., Evaluation of vegetation indices and modified simple ratio for boreal applications, Can. J. Remote Sens., 22, 229–242, 1996.

Coops, N. C., Stone, C., Culvenor, D. S., Chisholm, L. A., and Merton, R. N.: Chlorophyll content in eucalypt vegetation at the leaf and canopy scales as derived from high resolution spectral data, Tree Physiol., 23, 23–31, doi:10.1093/treephys/23.1.23, 2003.

Daughtry, C.: Estimating corn leaf chlorophyll concentration from leaf and canopy reflectance, Remote Sens. Environ., 74, 229–239, doi:10.1016/S0034-4257(00)00113-9, 2000.

Douglas, E. S., Strahler, A., Martel, J., Cook, T., Mendillo, C., Marshall, R., Chakrabarti, S., Schaaf, C., Woodcock, C., Li, Z., Yang, X., Culvenor, D., Jupp, D., Newnham, G., and Lovell, J.: DWEL: A Dual-Wavelength Echidna Lidar for ground-based forest scanning, in: IEEE Proceedings, International Geosciences And Remote Sensing Symposium 2012, Munich, Germany, 22–27 July, 4998–5001, 2012.

Gaulton, R., Danson, F. M., Ramirez, F. A., and Gunawan, O.: The potential of dual-wavelength laser scanning for estimating vegetation moisture content, Remote Sens. Environ., 132, 32–39, doi:10.1016/j.rse.2013.01.001, 2013.

Gond, V., de Pury, D. G. G., Veroustraete, F., and Ceulemans, R.: Seasonal variations in leaf area index, leaf chlorophyll, and water content; scaling-up to estimate fAPAR and carbon balance in a multilayer, multispecies temperate forest, Tree Physiol., 19, 673–679, doi:10.1093/treephys/19.10.673, 1999.

BGD
11, 15019–15035, 2014

Hakala, T., Suomalainen, J., Kaasalainen, S., and Chen, Y.: Full waveform hyperspectral LiDAR for terrestrial laser scanning, Opt. Express, 20, 7119, doi:10.1364/OE.20.007119, 2012.

Hancock, S., Lewis, P., Foster, M., Disney, M., and Muller, J.-P.: Measuring forests with dual wavelength lidar: a simulation study over topography, Agr. Forest Meteorol., 161, 123–133, doi:10.1016/j.agrformet.2012.03.014, 2012.

Jones, T. G., Coops, N. C., and Sharma, T.: Assessing the utility of airborne hyperspectral and LiDAR data for species distribution mapping in the coastal Pacific Northwest, Canada, Remote Sens. Environ., 114, 2841–2852, doi:10.1016/j.rse.2010.07.002, 2010.

Kaasalainen, S., Krooks, A., Liski, J., Raumonen, P., Kaartinen, H., Kaasalainen, M., Puttonen, E., Anttila, K., and Mäkipää, R.: Change detection of tree biomass with terrestrial laser scanning and quantitative structure modelling, Remote Sens., 6, 3906–3922, doi:10.3390/rs6053906, 2014.

Lausch, A., Heurich, M., Gordalla, D., Dobner, H.-J., Gwillym-Margianto, S., and Salbach, C.: Forecasting potential bark beetle outbreaks based on spruce forest vitality using hyperspectral remote-sensing techniques at different scales, Forest Ecol. Manag., 308, 76–89, doi:10.1016/j.foreco.2013.07.043, 2013.

Peltoniemi, M. S., Duursma, R. A., and Medlyn, B. E.: Co-optimal distribution of leaf nitrogen and hydraulic conductance in plant canopies, Tree Physiol., 32, 510–519, doi:10.1093/treephys/tps023, 2012.

Rouse, J. W., Haas, R. H., Schell, J. A., and Deering, W. D.: Monitoring vegetation systems in the Great Plains with ERTS, in: Third ERTS Symposium, NASA SP-351, 10–14 December 1973, Washington, D.C., 309–317, 1973.

Thomas, V., Finch, D. A., McCaughey, J. H., Noland, T., Rich, L., and Treitz, P.: Spatial modelling of the fraction of photosynthetically active radiation absorbed by a boreal mixedwood forest using a lidar–hyperspectral approach, Agr. Forest Meteorol., 140, 287–307, doi:10.1016/j.agrformet.2006.04.008, 2006.

Wang, L. and Schjoerring, J. K.: Seasonal variation in nitrogen pools and $^{15}N/^{13}C$ natural abundances in different tissues of grassland plants, Biogeosciences, 9, 1583–1595, doi:10.5194/bg-9-1583-2012, 2012.

Wellburn, A. R.: The Spectral Determination of Chlorophylls *a* and *b*, as well as Total Carotenoids, Using Various Solvents with Spectrophotometers of Different Resolution, J. Plant Physiol., 144, 307–313, doi:10.1016/S0176-1617(11)81192-2, 1994.

BGD
11, 15019–15035, 2014

Woodhouse, I. H., Nichol, C., Sinclair, P., Jack, J., Morsdorf, F., Malthus, T. J., and Patenaude, G.: A multispectral canopy LiDAR demonstrator project, IEEE Geosci. Remote S., 8, 839–843, doi:10.1109/LGRS.2011.2113312, 2011.

Wu, C., Niu, Z., Tang, Q., and Huang, W.: Estimating chlorophyll content from hyperspectral vegetation indices: modeling and validation, Agr. Forest Meteorol., 148, 1230–1241, doi:10.1016/j.agrformet.2008.03.005, 2008.

Zarco-Tejada, P. J., Miller, J. R., Noland, T. L., Mohammed, G. H., and Sampson, P. H.: Scaling-up and model inversion methods with narrowband optical indices for chlorophyll content estimation in closed forest canopies with hyperspectral data, IEEE T. Geosci. Remote, 39, 1491–1507, doi:10.1109/36.934080, 2001.

BGD
11, 15019–15035, 2014

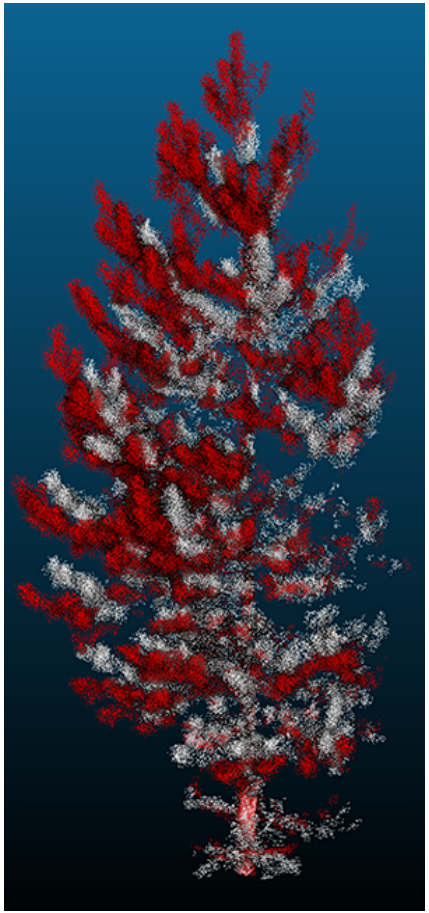

Figure 1. Co-registered point clouds from 15 May 2013 scan (grey) and 6 November 2013 scan (red). Growth of the tree is visible and also some movement of the branches can be observed.

BGD
11, 15019–15035, 2014

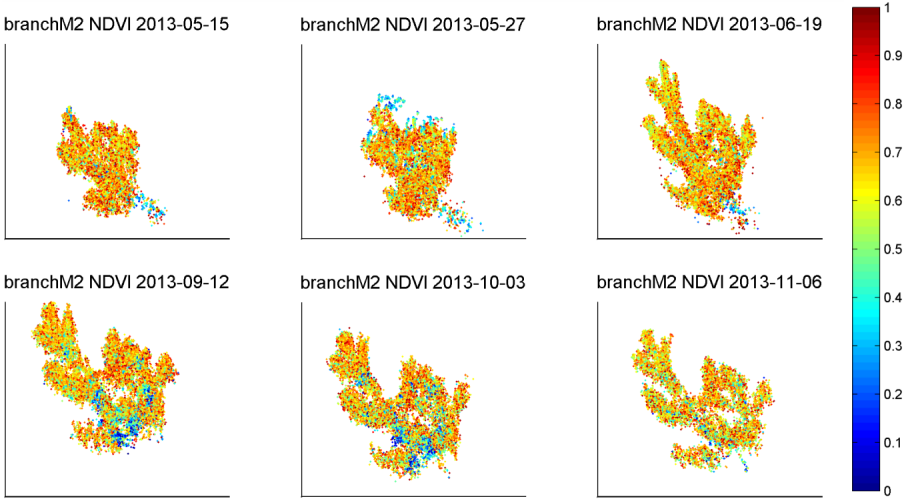

Figure 2. NDVI (see the colour bar for values) point clouds of a sample branch M2. The growth of new needles (starting 27 May), already clearly visible new branch tips 19 June, fully grown new needles 12 September and dying and falloff of old needles (shown in bluish green colours in 12 September and 3 October) are visible in the data measured at different times. The measurement dates are shown in the plot titles.

BGD
11, 15019–15035, 2014

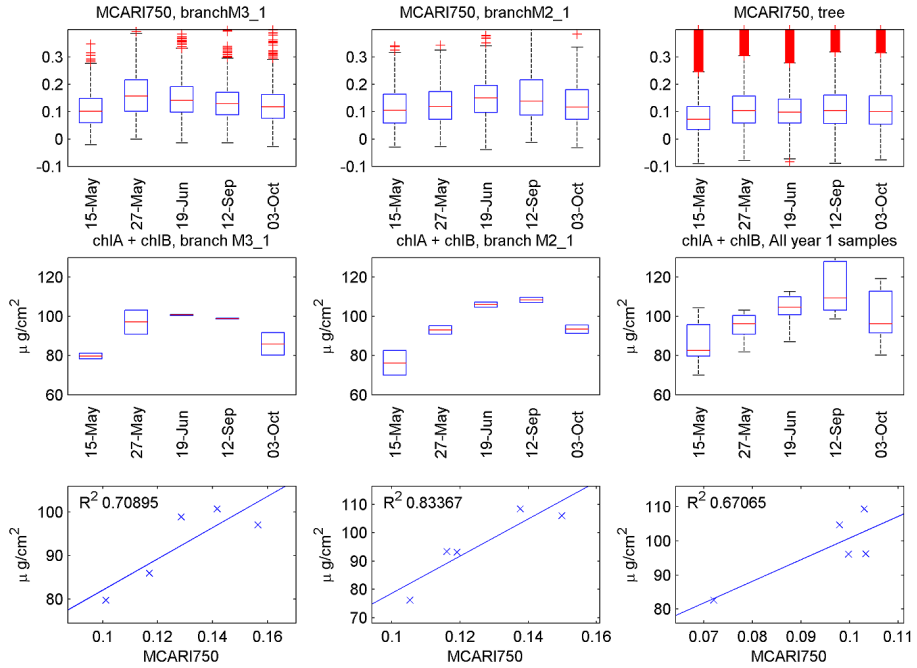

Figure 3. Top row: distribution of MCARI750 spectral index during separate HSL measurements, the central mark is the median, the edges of the box are the 25th and 75th percentiles, the whiskers extend to the most extreme data points not considered outliers. Middle row: laboratory measurements chlorophyll $a + b$. Bottom row: correlation of the spectral index and laboratory measurement. Subplot columns left to right: sample branch 3 year 1, sample branch 2 year 1, spectral index of whole tree and laboratory measurements of all year 1 samples.

BGD
11, 15019–15035, 2014

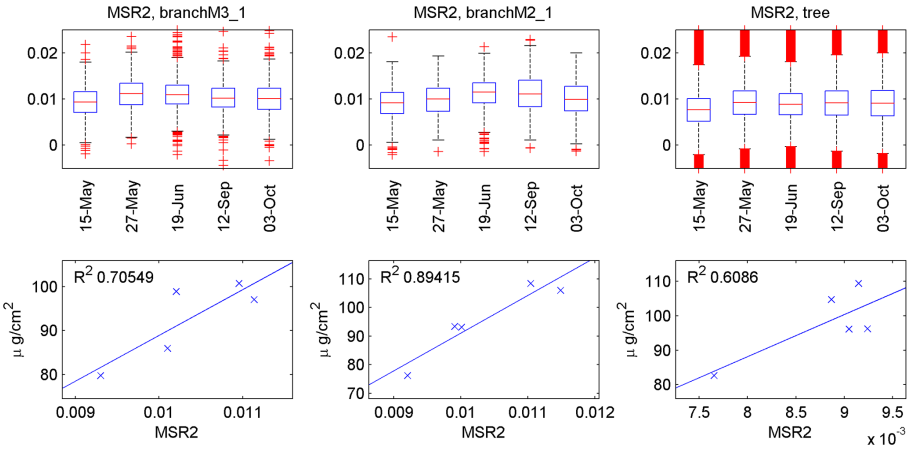

Figure 4. Same as previous figure (top and bottom rows, laboratory data is the same as in previous figure), this time using MSR2 spectral index.

BGD
11, 15019–15035, 2014

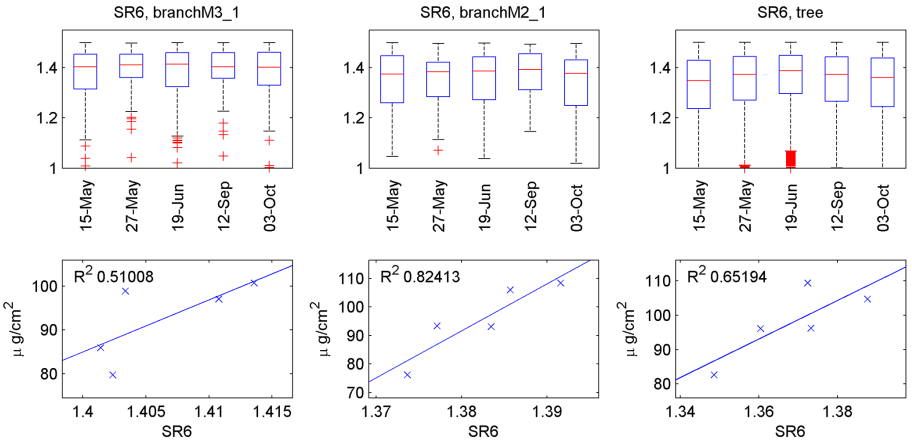

Figure 5. Same as previous figure, this time using SR6 spectral index.

BGD
11, 15019–15035, 2014

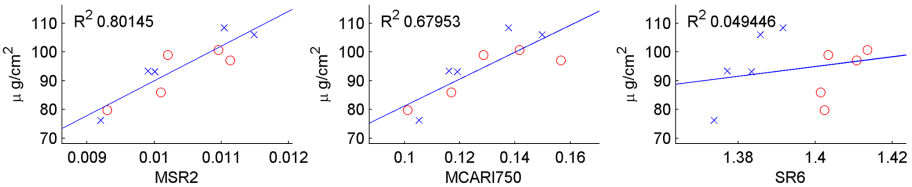

Figure 6. Correlation of spectral index and laboratory measurement for combined M2_1 and M3_1 data. Left: MSR2, middle: MCARI750, right: SR6. Blue x: M3_1, red circle: M2_1.

BGD
11, 15019–15035, 2014